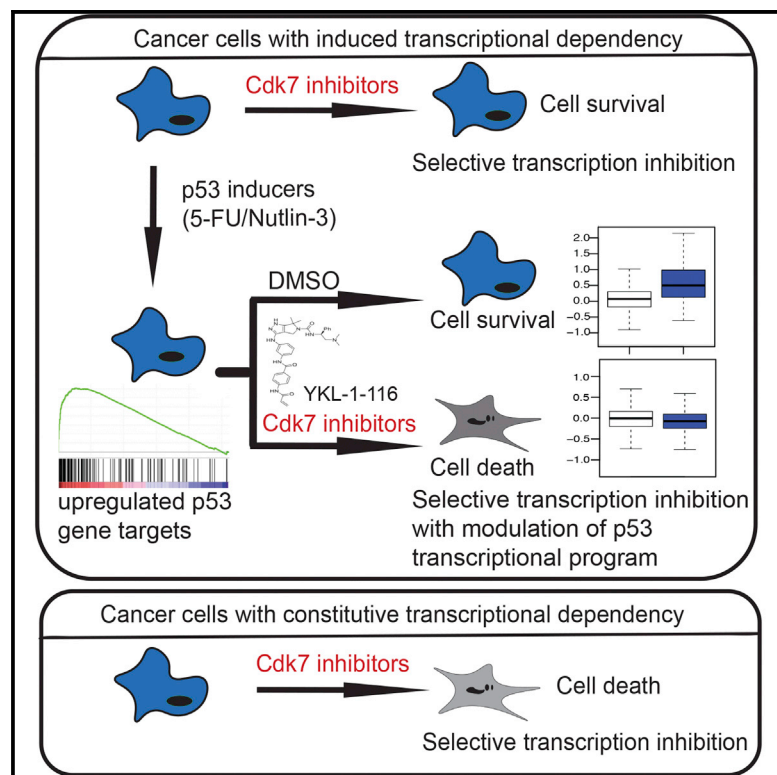


Activation of the p53 Transcriptional Program Sensitizes Cancer Cells to Cdk7 Inhibitors

Graphical Abstract



Authors

Sampada Kalan, Ramon Amat, Miriam Merzel Schachter, ..., Richard A. Young, Nathanael S. Gray, Robert P. Fisher

Correspondence

robert.fisher@mssm.edu

In Brief

Kalan et al. find that activation of the p53 tumor suppressor protein in human colon cancer-derived cells can induce transcriptional dependency on Cdk7, analogous to constitutive dependencies described in other tumors driven by oncogenic transcription factors. This work provides a proof of concept for combining p53-activating agents with Cdk7 inhibitors to elicit synthetic lethality.

Highlights

- Cdk7 inhibition plus p53 activation cause synthetic lethality in cancer cells
- Chemical genetics lead to the discovery of synthetic-lethal drug combinations
- Synergy with p53 activators is enhanced by increasing selectivity of the Cdk7 inhibitor
- Cdk7 inhibition modulates p53 transcriptional program to favor pro-apoptotic targets



Activation of the p53 Transcriptional Program Sensitizes Cancer Cells to Cdk7 Inhibitors

Sampada Kalan,^{1,6} Ramon Amat,^{1,6} Miriam Merzel Schachter,¹ Nicholas Kwiatkowski,^{2,3} Brian J. Abraham,⁴ Yanke Liang,^{2,3} Tinghu Zhang,^{2,3} Calla M. Olson,^{2,3} Stéphane Larochelle,¹ Richard A. Young,^{4,5} Nathanael S. Gray,^{2,3} and Robert P. Fisher^{1,7,*}

¹Department of Oncological Sciences, Icahn School of Medicine at Mount Sinai, New York, NY 10029, USA

²Department of Cancer Biology, Dana-Farber Cancer Institute, Boston, MA 02115, USA

³Department of Biological Chemistry and Molecular Pharmacology, Harvard Medical School, Boston, MA 02115, USA

⁴Whitehead Institute for Biomedical Research, Cambridge, MA 02142, USA

⁵Department of Biology, Massachusetts Institute of Technology, MA 02142, USA

⁶These authors contributed equally

⁷Lead Contact

*Correspondence: robert.fisher@mssm.edu

<https://doi.org/10.1016/j.celrep.2017.09.056>

SUMMARY

Cdk7, the CDK-activating kinase and transcription factor IIH component, is a target of inhibitors that kill cancer cells by exploiting tumor-specific transcriptional dependencies. However, whereas selective inhibition of analog-sensitive (AS) Cdk7 in colon cancer-derived cells arrests division and disrupts transcription, it does not by itself trigger apoptosis efficiently. Here, we show that p53 activation by 5-fluorouracil or nutlin-3 synergizes with a reversible Cdk7^{as} inhibitor to induce cell death. Synthetic lethality was recapitulated with covalent inhibitors of wild-type Cdk7, THZ1, or the more selective YKL-1-116. The effects were allele specific; a *CDK7^{as}* mutation conferred both sensitivity to bulky adenine analogs and resistance to covalent inhibitors. Non-transformed colon epithelial cells were resistant to these combinations, as were cancer-derived cells with p53-inactivating mutations. Apoptosis was dependent on death receptor DR5, a p53 transcriptional target whose expression was refractory to Cdk7 inhibition. Therefore, p53 activation induces transcriptional dependency to sensitize cancer cells to Cdk7 inhibition.

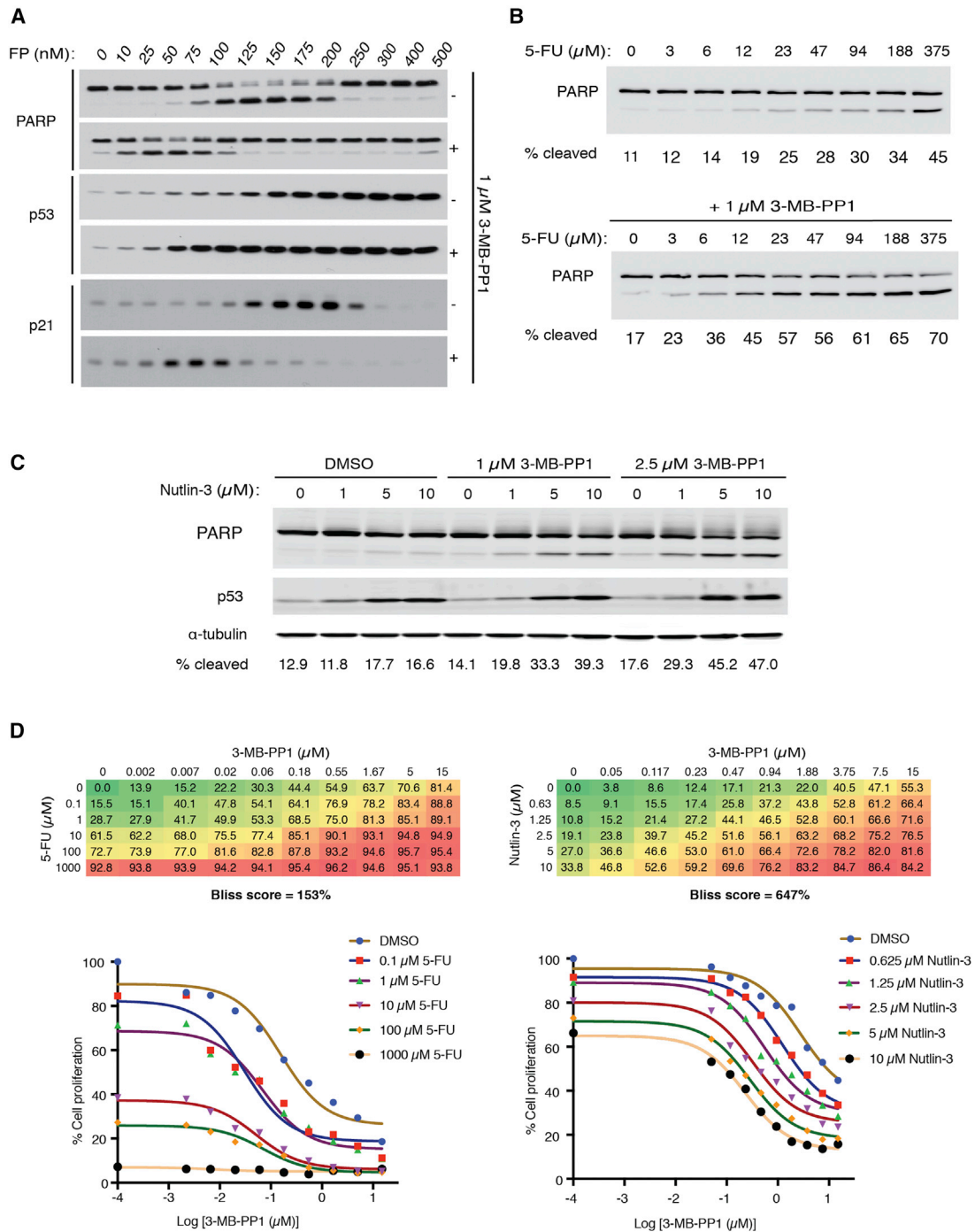
INTRODUCTION

Cyclin-dependent kinases (CDKs) regulate eukaryotic cell division and RNA polymerase II (Pol II)-dependent transcription (reviewed in [Morgan, 2007](#) and [Sansó and Fisher, 2013](#)). Cdk7 plays essential, direct roles in both cell division and transcription cycles, as a CDK-activating kinase (CAK) that phosphorylates CDKs on the activation segment (T loop) and as part of general transcription factor (TF) IIH (reviewed in [Fisher, 2005](#)). Physiologic functions and targets of Cdk7 have been identified by a chemical-genetic, “bumped-hole” approach—ATP-binding site expansion by mutation of the gatekeeper residue to accommo-

date bulky inhibitors or substrate analogs that cannot bind wild-type kinases ([Bishop et al., 1998](#)). Gene targeting to replace Cdk7^{WT} with an analog-sensitive (AS) mutant version allowed selective inhibition of the endogenous kinase in human colon cancer-derived HCT116 cells ([Larochelle et al., 2007](#)).

As a CAK, Cdk7 is inherently able to influence both cell division and gene expression; T loop phosphorylation is required for the functions of both cell-cycle and transcriptional CDKs ([Larochelle et al., 2012](#); [Schachter et al., 2013](#)). Apart from its CAK function, Cdk7, working in the context of TFIIH, phosphorylates the C-terminal domain (CTD) of the Pol II large subunit Rpb1, with a preference for Ser5 and Ser7 positions of the heptad repeat consensus sequence, Y₁S₂P₃T₄S₅P₆S₇ ([Ramathan et al., 2001](#); [Glover-Cutter et al., 2009](#)). Cdk7 activity is needed for the promoter-proximal pause, a rate-limiting step in expression of genes transcribed by Pol II ([Adelman and Lis, 2012](#)). Cdk7 promotes recruitment of the 5,6-dichloro-1-β-D-ribofuranosyl-benzimidazole (DRB) sensitivity-inducing factor (DSIF) and negative elongation factor (NELF) to the transcription complex ([Glover-Cutter et al., 2009](#); [Larochelle et al., 2012](#)), which throws up a block to elongation that is relieved by positive transcription elongation factor b (P-TEFb) ([Peterlin and Price, 2006](#)). P-TEFb is itself a CDK, consisting of Cdk9 and cyclin T1, activation of which depends on phosphorylation by Cdk7 ([Larochelle et al., 2012](#)). Therefore, Cdk7 acts both to establish and to overcome the pause imposed by DSIF and NELF; loss of this regulation diminishes Pol II occupancy in gene bodies, and it is likely to uncouple RNA synthesis and co-transcriptional processing ([Glover-Cutter et al., 2009](#); [Larochelle et al., 2012](#)).

Despite extensive efforts to target cell-cycle CDKs for anti-cancer therapy ([Malumbres and Barbacid, 2009](#)), parallel approaches aimed at transcriptional CDKs only recently gained traction. A covalent inhibitor of Cdk7, THZ1, induced global transcriptional shutdown at high doses, but it had gene-selective repressive effects at lower doses ([Kwiatkowski et al., 2014](#)). In vitro, THZ1 recapitulated effects of Cdk7 inhibition on Pol II pausing, and it impaired co-transcriptional RNA 5' end capping ([Nilson et al., 2015](#)). Moreover, THZ1 triggered apoptosis of sensitive cells in culture, and it limited or reversed growth of



(legend continued on next page)

specific tumors—T cell acute lymphoblastic leukemia (T-ALL), neuroblastoma, small cell lung cancer (SCLC), and triple-negative breast cancer (TNBC)—with minimal toxicity in human xenograft mouse models (Chipumuro et al., 2014; Christensen et al., 2014; Kwiatkowski et al., 2014; Wang et al., 2015).

Here, we show that selective inhibition of Cdk7 in HCT116 cells does not by itself trigger apoptosis, but it potentiates p53-dependent cell killing by the antimetabolite 5-fluorouracil (5-FU), and it switches cell fate from division arrest to death upon p53 stabilization by nutlin-3. These synthetic-lethal effects were (1) recapitulated with covalent inhibitors of transcriptional CDKs, such as THZ1 or the more Cdk7-selective YKL-1-116, in wild-type cells; (2) dependent on wild-type p53 function and ongoing transcription; and (3) accompanied by caspase 8 activation and suppressed by depletion of the death receptor (and p53 target) DR5, suggesting engagement of the extrinsic apoptotic pathway (Henry et al., 2012). Previous studies reported lethality due to combined inhibition of poly(ADP-ribose) polymerase (PARP) and CDKs implicated in DNA damage responses (Johnson et al., 2011, 2016). We provide proof of concept for synthetic-lethal strategies targeting CDK functions in p53-responsive transcription.

RESULTS

Inhibition of Multiple CDKs Promotes Apoptosis

To dissect Cdk7 functions *in vivo*, we previously replaced both wild-type copies of *CDK7* with *CDK7^{F91G/D92E}* (*CDK7^{as}*) in HCT116 cells (Larochelle et al., 2007). Treatment of these cells with bulky adenine analogs such as 3-MB-PP1, which potently inhibits Cdk7^{as} *in vitro*, prevented T loop phosphorylation of Cdk1, -2, -4, -6, and -9, and it led to cell-cycle arrests and transcription defects (Larochelle et al., 2007, 2012; Glover-Cutter et al., 2009; Schachter et al., 2013). However, it did not efficiently induce apoptosis, measured by PARP cleavage, the accumulation of annexin V-positive cells, or caspase activation (Figures S1A–S1C). This is in contrast to the pro-apoptotic effects of THZ1 in T-ALL and other sensitive cell types (Kwiatkowski et al., 2014).

We considered two possible, but not mutually exclusive, explanations for the difference. First, THZ1 might elicit apoptosis through the inhibition of Cdk7 and additional targets in the same pathway, such as Cdk12 and/or Cdk13 (Kwiatkowski et al., 2014). Second, vulnerability to selective CDK inhibitors might be based on transcriptional dependencies unique to certain cancers but lacking in HCT116 cells. To explore the first possibility, we treated *CDK7^{as/as}* cells with increasing doses of 3-MB-PP1 in the absence or presence of flavopiridol (FP), a pan-CDK inhibitor that is most potent toward Cdk9 but that also inhibits Cdk12 at higher doses (Chao and Price, 2001; Böskén et al., 2014; Bartkowiak and Greenleaf, 2015). The addition of sublethal doses of FP (10 or 50 nM) sensitized cells to killing by Cdk7 inhibition. However, 3-MB-PP1 doses >2 μ M

suppressed PARP cleavage in the presence of 50 nM FP, and, at 150 nM FP (a lethal dose on its own in *CDK7^{as/as}* cells), 3-MB-PP1 suppressed PARP cleavage at doses >100 nM (Figure S1A).

Similarly, the response of *CDK7^{as/as}* cells to FP alone was biphasic, with a maximum at \sim 125 nM and suppression at \geq 250 nM (Figure 1A). Expression of p53 increased after FP treatment with half-maximal induction at \sim 150 nM, within the pro-apoptotic range. The addition of 1 μ M 3-MB-PP1 shifted the FP dose needed for maximal PARP cleavage to \sim 50 nM. At higher doses of FP, apoptosis was suppressed; PARP cleavage returned to background levels at 125 nM, the optimal dose in the absence of 3-MB-PP1. Cdk7 inhibition similarly potentiated FP effects on p53 expression, which remained elevated as the FP dose was raised. In contrast, a p53 transcriptional target—the CDK inhibitor p21—was induced over a narrow FP dose range, which was roughly co-extensive with the pro-apoptotic range and likewise shifted to lower doses by 3-MB-PP1 addition. Therefore, simultaneous inhibition of multiple CDKs can induce apoptosis in HCT116 cells, but biphasic responses imply a limitation on the ability of broad-specificity CDK inhibitors to trigger cell death; at higher concentrations these drugs lose efficacy, possibly because they also block transcription of pro-apoptotic p53 targets.

Cdk7 Inhibition Potentiates Cell Killing by p53-Activating Agents

FP elicited a p53 response and cell death, which were potentiated by a Cdk7-selective drug that by itself did not activate p53. At lower doses, where it is more likely to be Cdk7 selective, THZ1 triggered apoptosis in vulnerable tumor cells with fixed dependencies on oncogenic transcription factors (Kwiatkowski et al., 2014). We reasoned that p53-activating agents might induce a similar dependency and, because they do not directly target the CDK network, do so without the dose limitation seen with FP. We tested 5-FU and nutlin-3, which elicit different p53-dependent phenotypes—death or arrested division, respectively—in HCT116 cells (Donner et al., 2007). In *CDK7^{as/as}* cells, Cdk7 inhibition potentiated the effect of 5-FU by \sim 20-fold; half-maximal PARP cleavage occurred at \sim 20 μ M 5-FU in the presence of 1 μ M 3-MB-PP1, compared to >300 μ M in its absence (Figure 1B). Similarly, treatment of *CDK7^{as/as}* cells with 1–10 μ M nutlin-3 alone did not trigger apoptosis, but it did so when combined with 3-MB-PP1 (Figure 1C). Combination of either 5-FU or nutlin-3 with 3-MB-PP1 led to a greater-than-additive accumulation of annexin V-positive cells, and both PARP cleavage and annexin V staining could be blocked by the addition of the caspase inhibitor Z-VAD (Figures S1B and S1C). There was no difference in levels of p53 induced by nutlin-3 in the presence or absence of 3-MB-PP1, indicating that Cdk7 inhibition works downstream of p53 to switch cell fate from division arrest to death in response to nutlin-3.

(D) Bliss independence analysis in *CDK7^{as/as}* cells for 3-MB-PP1 and 5-FU (left) or nutlin-3 (right). Bliss scores were calculated from mean values of full concentration matrices performed in triplicate. Numbers in matrices indicate percentage reduction in metabolic activity, as measured by resazurin staining, relative to DMSO-treated cells. Growth inhibition curves derived from these data are shown below each matrix.

See also Figure S1.

We tested for synergy between 3-MB-PP1 and p53-activating agents by combination analysis over full concentration matrices (Figure 1D). The analog acted synergistically to shift dose responses to 5-FU and, to a greater extent, nutlin-3, as indicated by strongly positive Bliss independence scores (Zhao et al., 2014). Cdk7 inhibition therefore lowers 5-FU doses needed to kill tumor cells that are normally responsive to the drug, and it confers nutlin-3 sensitivity on normally resistant cells. These results suggest that p53 stabilization might induce transcriptional dependency, sensitizing cells to killing by single-CDK inhibition.

Synthetic Lethality of p53 Activators with Covalent Inhibitors of Wild-Type Cdk7

We next asked if synthetic-lethal effects of 3-MB-PP1 in $CDK7^{as/as}$ cells could be recapitulated with THZ1. Modeling of THZ1 docked with an X-ray crystal structure of human Cdk7 suggested close proximity of the drug to the side chain of gate-keeper residue Phe91 (Kwiatkowski et al., 2014). In vitro, $Cdk7^{as}$ complexes were resistant to THZ1 at concentrations up to 10 μ M (Figure 2A). In contrast, $Cdk7^{WT}$ was inhibited by THZ1 with an IC_{50} of \sim 100 nM. Conversely, $Cdk7^{WT}$ was insensitive to 3-MB-PP1, which inhibited $Cdk7^{as}$ with an IC_{50} of \sim 10 nM, as reported (Merrick et al., 2008).

We tested the allele specificity of each drug in wild-type and $CDK7^{as/as}$ cells (Figure 2B). In the absence of other drugs, neither 10–100 nM THZ1 nor 0.5–2.5 μ M 3-MB-PP1 induced PARP cleavage in either genetic background (although 100 nM THZ1 induced p53 expression in wild-type cells). When combined with 40 μ M 5-FU, THZ1 induced PARP cleavage in $CDK7^{WT/WT}$ cells, but only at doses of 10 and 50 nM and not at 100 nM. In $CDK7^{as/as}$ cells, however, there was no synthetic-lethal effect of combining 5-FU and THZ1. As expected, 3-MB-PP1 had the opposite allele specificity—synthetic lethality with 5-FU in $CDK7^{as/as}$, but not in $CDK7^{WT/WT}$, cells—with no loss of efficacy at higher doses.

In deriving $CDK7^{as/as}$ cells, we generated heterozygous, $CDK7^{WT/as}$ intermediates (Larochelle et al., 2007), which express wild-type and AS Cdk7 at approximately equal levels and, therefore, should retain Cdk7 activity in the presence of either 3-MB-PP1 or THZ1, but not both drugs. In accordance with this prediction, $CDK7^{WT/as}$ cells did not undergo apoptosis when treated with pairwise combinations of 5-FU and either 3-MB-PP1 or THZ1, but they did so when all three drugs were added (Figure 2B). Therefore, a single copy of either $CDK7$ allele, wild-type (WT) or as, can complement inactivation of the enzyme encoded by the other. This further validates Cdk7 as the unique, common target of 3-MB-PP1 and THZ1 relevant for synthetic lethality.

Synthetic Lethality of 5-FU and CDK Inhibitors Is p53 Dependent

We hypothesized that p53 stabilization establishes dependency on Cdk7, such that Cdk7 inhibition modifies the downstream transcriptional response to favor pro-apoptotic over pro-survival pathways. It follows that synthetic lethality should depend on a functional p53. To test that prediction, we used recombinant adeno-associated virus (rAAV) vectors (Topaloglu et al., 2005)

to disrupt both copies of $TP53$ (encoding p53) in $CDK7^{as/as}$ HCT116 cells (Figure S2A). In $CDK7^{as/as} TP53^{-/-}$ cells, neither p53 nor p21 was detectable after treatment with the DNA-damaging agent doxorubicin, whereas both were induced in $CDK7^{as} TP53^{+}$ cells (Figure S2B). Loss of p53 led to a slight sensitization to 3-MB-PP1, measured either by PARP cleavage or cell viability (Figures 2C and S2C). The effects of combined 3-MB-PP1 and 5-FU treatment were less than additive, however, in $CDK7^{as/as} TP53^{-/-}$ cells (Figures 2C and S2D). (The $CDK7^{as}$ mutation also appeared to sensitize $TP53^{-/-}$ cells to treatment with 375 μ M 5-FU [Figure S2E].) Similarly, we observed greater-than-additive effects of combining 5-FU with THZ1 in $TP53^{+/+}$, but not in $TP53^{-/-}$, HCT116 cells with wild-type Cdk7 (Figure 2D) and in $TP53^{+}$ colorectal cancer-derived RKO (Figure S2F) or LoVo cells (data not shown), but not in the $TP53^{-}$ mutant lines HT29 or DLD1 (Figure S2G). Therefore, the synthetic lethality of 5-FU + Cdk7 inhibition in colon cancer-derived cells depends on an intact p53 pathway.

A Cdk7-Selective Covalent Inhibitor Synergizes with 5-FU and Nutlin-3

By analogy with the biphasic response to FP (Figure 1A), we suspected that attenuated synthetic lethality at THZ1 doses $>$ 50 nM (Figure 2B) might be due to the inhibition of additional THZ1 targets, such as Cdk12 and Cdk13 (Kwiatkowski et al., 2014). The response of $CDK7^{as/as}$ cells to 3-MB-PP1 was not similarly biphasic, so we reasoned that a more selective inhibitor of wild-type Cdk7 might work over a broader dose range. As part of efforts to develop more specific kinase inhibitors, we synthesized YKL-1-116 (Figure 3A), a covalent inhibitor of Cdk7 (Figures S3A and S3B) that does not target Cdk9, Cdk12, or Cdk13 (Figure 3B; Tables S1 and S2). In vitro, YKL-1-116 was more potent than THZ1 toward both $Cdk7^{WT}$ and $Cdk7^{as}$, although $Cdk7^{as}$ was relatively resistant to this compound as well (Figure 3C). In wild-type cells, YKL-1-116 alone elicited minimal amounts of PARP cleavage only at the highest doses tested, reminiscent of the effects of 3-MB-PP1 on $CDK7^{as/as}$ cells. In combination with 40 μ M 5-FU, however, YKL-1-116 induced PARP cleavage in a dose-dependent fashion, with little loss of efficacy at higher concentrations (Figure 3D). Similarly, combining 5 μ M nutlin-3 with 100–800 nM YKL-1-116 produced dose-dependent increases in PARP cleavage (Figure 3E). As with THZ1, synthetic lethality depended on potency toward Cdk7: the $CDK7^{as/as}$ cells were resistant to combinations of YKL-1-116 and either 5-FU (Figure 3D) or nutlin-3 (Figure 3E). Moreover, both 5-FU and nutlin-3 shifted dose responses of wild-type cells to YKL-1-116, with strongly positive Bliss scores indicating drug synergy (Figure 3F). Similar independence analysis of THZ1 yielded weakly positive or even negative scores due to a loss of efficacy at higher doses (data not shown). Combinations of YKL-1-116 with either 5-FU or nutlin-3 were effective against a variety of p53-positive cells derived from different tumor types (Figures S3C–S3F). Finally, combinations of THZ1 or YKL-1-116 with 5-FU did not trigger PARP cleavage in a non-transformed colorectal epithelial cell line, CCD 841 CoN, despite the induction of p53 (Figure S3G). Taken together, the results with 3-MB-PP1, THZ1, and YKL-1-116 indicate that increasing the specificity of Cdk7 inhibition can enhance synergistic,

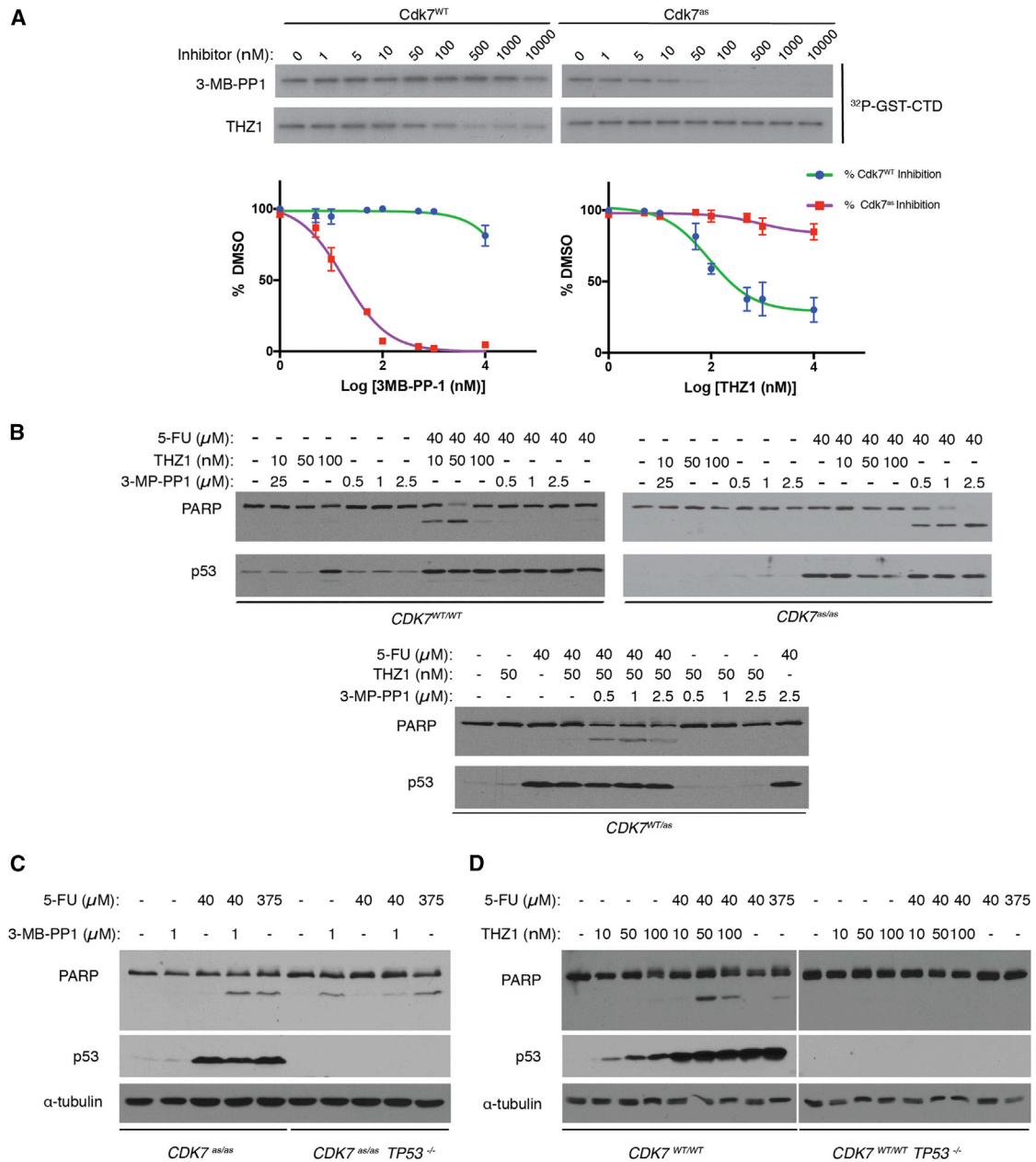


Figure 2. Synthetic Lethality of 5-FU and Cdk7 Inhibitors Is CDK7 Allele Specific and p53 Dependent

(A) Allele-specific inhibition of Cdk7 in vitro. T loop-phosphorylated, trimeric complexes containing Cdk7 (WT or as), cyclin H, and Mat1 (~5 nM each) were incubated with the indicated concentrations of 3-MB-PP1 or THZ1, and they were tested for kinase activity toward a fusion protein containing the Pol II CTD (GST-CTD), with results shown by representative autoradiograms (top) and quantified by Phosphorimager (bottom). Error bars indicate ± SEM of triplicate samples.

(B) CDK7^{WT/WT}, CDK7^{as/as}, or CDK7^{WT/as} HCT116 cells, as indicated, were treated with the indicated combinations and doses of drugs for 14 hr prior to extract preparation and immunoblot detection of PARP and p53.

(C) CDK7^{as/as} TP53^{-/-} HCT116 cells were treated with the indicated drugs, at the indicated doses, for 14 hr prior to lysis and immunoblot detection of PARP, p53, and α-tubulin.

(D) Wild-type or TP53^{-/-} HCT116 cells were treated with the indicated drugs, at the indicated doses, for 14 hr prior to lysis and immunoblot detection of PARP, p53, and α-tubulin.

See also Figure S2.

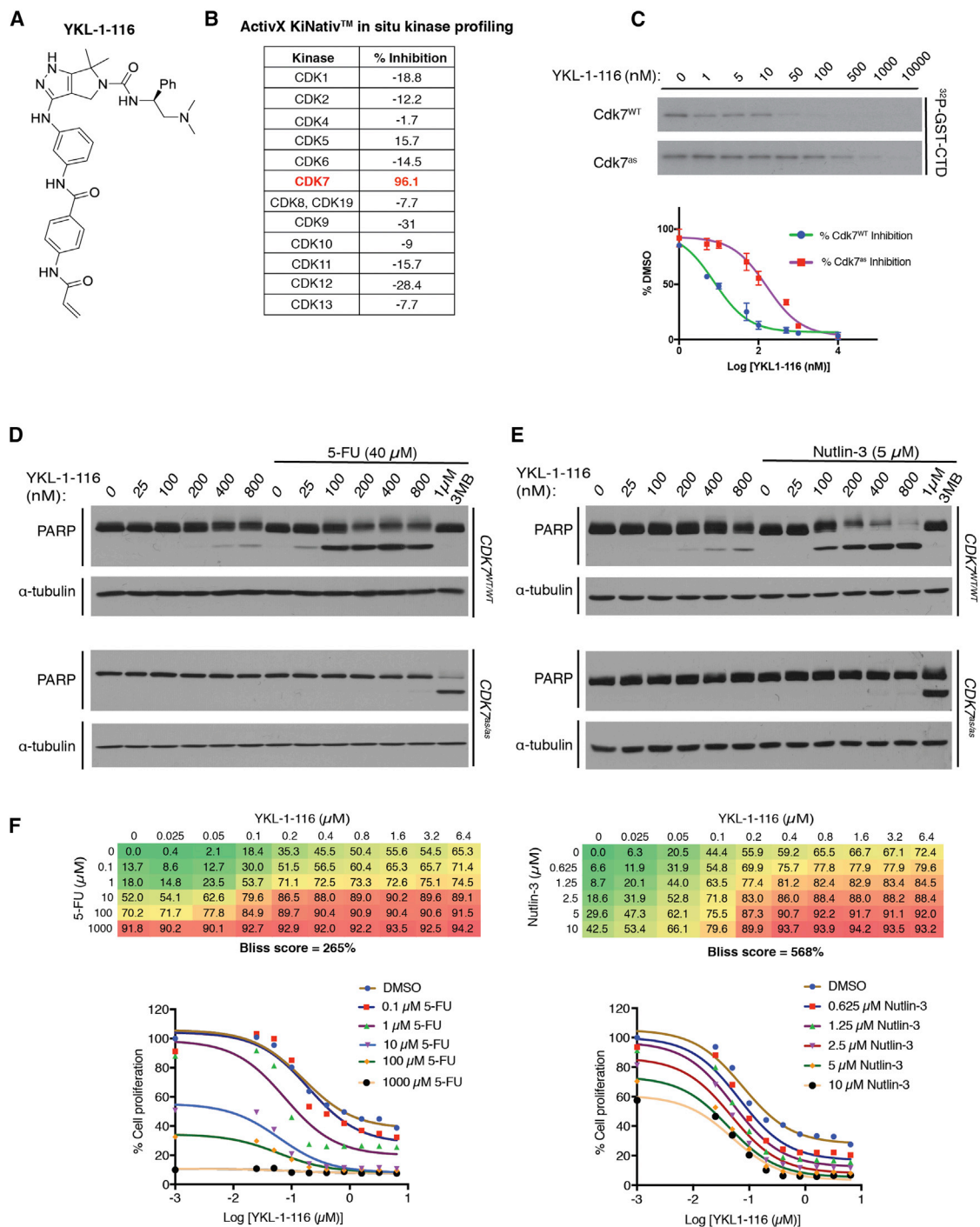


Figure 3. YKL-1-116, a Cdk7-Selective Covalent Inhibitor, Synergizes with 5-FU or Nutlin-3 to Kill HCT116 Cells

(A) YKL-1-116 structure.

(B) Selectivity of YKL-1-116 for Cdk7 over other CDKs, as determined by KiNativ kinome profiling. For each CDK, the percentage inhibition of labeling by a desthiobiotin-ATP probe after exposure in vivo to YKL-1-116 is indicated.

(C) Inhibition of Cdk7 by YKL-1-116 in vitro. As in Figure 2A, complexes containing Cdk7 (WT or as) were incubated with the indicated concentrations of YKL-1-116 and tested for kinase activity toward GST-C1D, with results shown by representative autoradiograms (top) and quantified by Phosphorimager (bottom). Error bars indicate \pm SEM of triplicate samples.

(D) $CDK7^{WT/WT}$ or $CDK7^{as/as}$ HCT116 cells were treated with the indicated Cdk7 inhibitors, at the indicated doses, with or without 40 μ M 5-FU, as indicated, for 14 hr prior to lysis and immunoblot detection of PARP and α -tubulin.

(legend continued on next page)

synthetic-lethal effects of combinatorial treatments in cancer-derived cells with functional p53.

Transcriptional Disruption Underlies Synthetic Lethality of 5-FU and Cdk7 Inhibition

To unravel the mechanism(s) of this synthetic lethality, we first compared the effects of FP, which at low doses primarily affects transcriptional CDKs, and purvalanol A, which inhibits cell-cycle CDKs activated by Cdk7, with selectivity for Cdk1 (Gray et al., 1998). In wild-type HCT116 cells, which are less FP sensitive than *CDK7^{as/as}* cells (Larochelle et al., 2012), 150 nM FP did not induce PARP cleavage on its own, but it did so in combination with sublethal doses of 5-FU (Figure S4A). In contrast, there was no detectable PARP cleavage after treatment with 5-FU and purvalanol A. There was likewise no PARP cleavage in 5-FU-exposed *CDK2^{as/as}* HCT116 cells treated with 3-MB-PP1 (Figure S4B), which impedes G1/S progression by inhibiting Cdk2^{as} in these cells (Merrick et al., 2011). We infer that CDK functions in transcription are needed to avoid apoptosis after 5-FU exposure. Also suggestive of a transcription-dependent mechanism, synthetic lethality could be suppressed by simultaneous treatment with triptolide (Figure 4A), which covalently inhibits XPB, a TFIIH subunit required for transcription by Pol II (Titov et al., 2011). In contrast, specific inhibitors of Pol I or Pol III—CX5461 (Drygin et al., 2011) or ML60218 (Wu et al., 2003), respectively—were unable to suppress synthetic lethality, even when added together. Therefore, Pol II activity is necessary and sufficient for the transcription-dependent lethality of combined 5-FU treatment and Cdk7 inhibition.

5-FU can be incorporated into DNA or RNA (Longley et al., 2003). Therefore, to test if synthetic lethality depended on RNA or DNA metabolism, we compared the effects of ribose or deoxyribose derivatives of 5-FU—5-fluorouridine (5-FUR) or 5-fluoro-2'-deoxyuridine (5-FdUR), respectively (Figures 4B and 4C). Even in the absence of 3-MB-PP1, *CDK7^{as/as}* HCT116 cells were more sensitive to 5-FUR than to 5-FU or 5-FdUR. The addition of 1 μ M 3-MB-PP1 potentiated pro-apoptotic effects of 5-FUR, but not 5-FdUR, suggesting that the relevant toxic metabolite is 5-FU-containing RNA rather than DNA.

Prior Exposure to 5-FU Sensitizes Cells to Cdk7 Inhibition

To dissect these responses further, we first determined when *CDK7^{as/as}* HCT116 cells exposed to various treatments became committed to apoptosis. In cells treated with 5 μ M nutlin-3 + 2.5 μ M 3-MB-PP1 or with 375 μ M 5-FU alone, PARP cleavage measured at 24 hr was largely, but not completely, prevented if drugs were removed as late as 12 hr after addition. In contrast, combined treatment with 40 μ M 5-FU and 2.5 μ M 3-MB-PP1 accelerated passage of a point of no return; cells became irre-

versibly committed to apoptosis 6–9 hr after drug addition (Figure 5A).

Nutlin-3 acts directly to inhibit ubiquitylation and proteasomal degradation of p53 (Vassilev et al., 2004). The mechanism of 5-FU action is indirect, requiring a toxic intermediate that, once it accumulates, can sustain p53 activation in the absence of the drug. Consistent with this scenario, we achieved similar cell-killing efficacy by simultaneous or sequential treatment with 5-FU and 3-MB-PP1, whereas nutlin-3 and 3-MB-PP1 needed to be administered together (Figure 5B). Moreover, the lethality of sequential treatment depended on the order of drug addition: 3-MB-PP1 was equally effective whether it was given with or after 5-FU treatment, and either regimen was more effective than 5-FU given only after 3-MB-PP1 removal.

The addition of 1 μ M triptolide during the first (5-FU) or second (3-MB-PP1) treatment suppressed PARP cleavage (Figure 5C). Rescue by triptolide after the removal of 5-FU indicates that ongoing Pol II transcription is required to activate caspases when Cdk7 is inhibited. Taken together with the relative toxicities of 5-FUR and 5-FdUR (Figures 4B and 4C), the results suggest that transcription is needed for both steps in the pathway leading to cell death, with a specific requirement for Pol II at the second, 3-MB-PP1-dependent step. Moreover, a time course of 3-MB-PP1 treatment after 5-FU washout indicated that the relevant differences in gene expression caused by Cdk7 inhibition would be detectable by 3–6 hr after the addition of 3-MB-PP1, when cells have committed to apoptosis but before effector caspases are activated (Figure 5D).

Cdk7 Inhibition Modulates the Transcriptional Response to p53 Activation

To detect alterations in transcription that might favor cell death when Cdk7 is inhibited, we performed RNA sequencing analysis (RNA-seq) of *CDK7^{as/as}* cells that were pre-treated with 40 μ M 5-FU or DMSO for 12 hr, washed, and incubated in fresh medium containing 2.5 μ M 3-MB-PP1 or DMSO for an additional 4 hr (Figure 6A). Treatment with 5-FU increased expression of 145 transcripts while repressing 420 genes (Figure 6B, left column). We asked if either of these transcript pools was enriched for known p53 targets included in the p53 Hallmark Pathway gene set (Broad Institute database MSigDB). Gene set enrichment analysis (GSEA) (Subramanian et al., 2005) revealed that members of this set were enriched among transcripts induced by 5-FU (Figure 6C). Expression of p53 targets was significantly elevated upon 5-FU treatment in comparison to changes in global mRNA levels (Figure 6D, top panel; Figure 6E, top panel). The addition of 3-MB-PP1 to 5-FU-treated cells blunted the induction of p53 targets relative to 5-FU treatment alone (Figure 6B, right column; Figure 6D, bottom panel; Figure 6E, bottom panel), although it did not restore expression of these genes to their pre-5-FU levels

(E) *CDK7^{WT/WT}* or *CDK7^{as/as}* HCT116 cells were treated with the indicated Cdk7 inhibitors, at the indicated doses, with or without 5 μ M nutlin-3, as indicated, for 14 hr prior to lysis and immunoblot detection of PARP and α -tubulin.

(F) Bliss independence analysis in *CDK7^{WT/WT}* cells for YKL-1-116 and 5-FU (left) or nutlin-3 (right). Bliss scores represent the mean of triplicate concentration matrices. Numbers in matrices indicate percentage reduction in metabolic activity, as measured by resazurin staining, relative to DMSO-treated cells. Growth inhibition curves derived from these data are shown below each matrix.

See also Figure S3 and Tables S1 and S2.

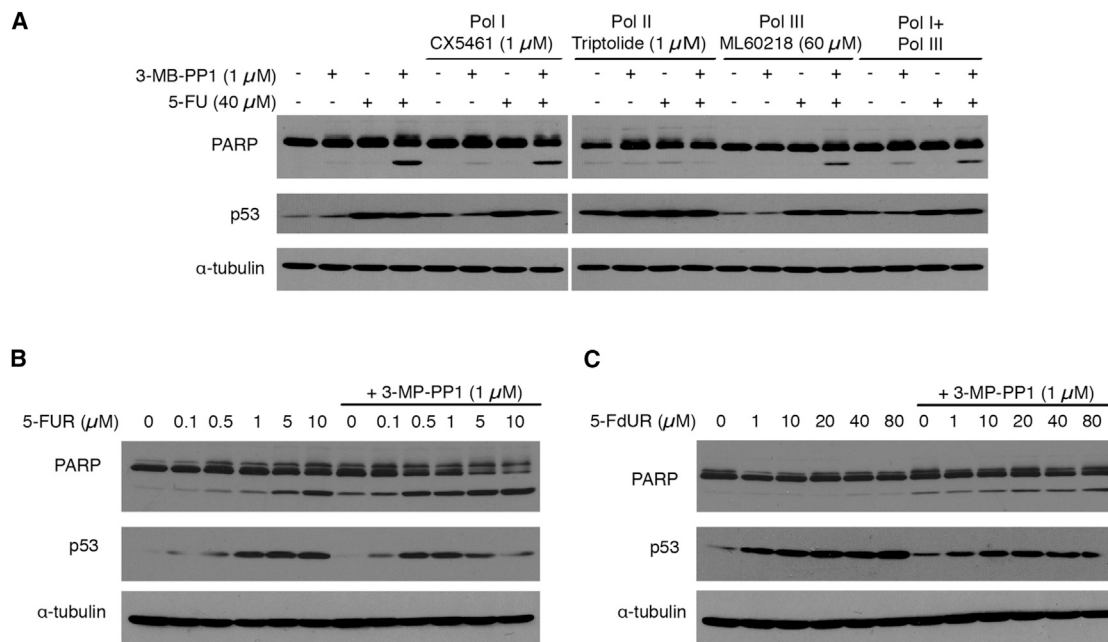


Figure 4. Synthetic Lethality of 5-FU + CDK Inhibition Is Transcription Dependent

(A) *CDK7^{as/as}* cells were treated with 5-FU (40 μ M) and/or 3-MB-PP1 (1 μ M), as indicated, with the addition of inhibitors of Pol I (1 μ M CX5461), Pol II (1 μ M triptolide), or Pol III (60 μ M ML60218), as indicated, for 14 hr prior to extract preparation and immunoblot detection of PARP, p53, and α -tubulin. (B) *CDK7^{as/as}* cells were treated with the indicated doses of 5-fluorouridine (5-FUR), without or with the addition of 1 μ M 3-MB-PP1, as indicated, for 14 hr prior to extract preparation and immunoblot detection of PARP, p53, and α -tubulin. (C) *CDK7^{as/as}* cells were treated with the indicated doses of 5-fluorodeoxyuridine (5-FdUR), without or with the addition of 1 μ M 3-MB-PP1, as indicated, for 14 hr prior to extract preparation and immunoblot detection of PARP, p53, and α -tubulin. See also Figure S4.

(Figure 6B, middle column; Figures S5A–S5C). Expression of p53-regulated genes such as *p21* and *MDM2* was reduced, suggesting attenuation of pro-survival transcriptional signaling induced by 40 μ M 5-FU (Figure 6F). We validated the decrease in *MDM2* transcripts by qRT-PCR analysis of cells treated simultaneously with 3-MB-PP1 and 5-FU (Figure 6G) or nutlin-3 (Figure 6H), and we verified that this change was dependent on the *CDK7^{as/as}* mutation (i.e., it did not occur in wild-type HCT116 cells; Figures S5D and S5E). Expression of Mdm2 and p21 proteins was also attenuated by Cdk7 inhibition, in response to sequential treatment with 5-FU and 3-MB-PP1 (Figures 6I and S5F) or simultaneous treatment with nutlin-3 and 3-MB-PP1 (Figures 6J and S5G).

In contrast to these effects on *MDM2* and *p21*, transcription levels of two pro-apoptotic p53 targets induced by 5-FU or nutlin-3—death receptor genes *DR5* and *FAS*—were sustained in the presence of 3-MB-PP1 (Figures 6F–6H). *DR5* and *FAS* proteins were also induced to similar levels by 5-FU or nutlin-3 in the absence or presence of 3-MB-PP1 (Figures 6I, 6J, S5F, and S5G). In cells pre-treated with DMSO, 3-MB-PP1 did not selectively affect the expression of p53-regulated genes, indicating that it specifically modulated transcriptional responses to p53 stabilization (Figures S5A–S5C). These results suggest that Cdk7 inhibitors might synergize with 5-FU or nutlin-3 by tipping the balance of p53-dependent transcription toward death-promoting targets such as *DR5* and *FAS*.

A Role for the Extrinsic Pathway and a Requirement for DR5 in Synthetic Lethality

The possible involvement of DR5 suggested engagement of the extrinsic pathway, which is implicated in HCT116 cell killing by higher doses of 5-FU (Henry et al., 2012). Effectors specific to the extrinsic pathway include caspase 8, which was activated by treating *CDK7^{as/as}* cells with 3-MB-PP1 in combination with either 5-FU (Figure 7A) or nutlin-3 (Figure 7B).

In HCT116 cells exposed to high-dose 5-FU, DR5 and FAS were previously shown to translocate to the plasma membrane, and DR5 silencing impeded caspase activation (Can et al., 2013). To assess the involvement of DR5, FAS, and DR4 (another death receptor) in synthetic lethality, we silenced the expression of each with small interfering RNA (siRNA), treated cells with 3-MB-PP1 and either 5-FU or nutlin-3, and measured markers of apoptosis. We achieved similar degrees of knockdown of each of the three proteins (Figures 7C, 7D, S6A, and S6B). Depletion of DR5 by \sim 50% diminished PARP cleavage and led to a statistically significant reduction in the annexin V-positive fraction ($p \approx 0.012$, two-tailed t test) in cells treated with 3-MB-PP1 + 5-FU (Figures 7C and 7E) and a reproducible reduction in cells treated with 3-MB-PP1 + nutlin-3 (Figures 7D and 7F). Knockdown of FAS also caused a significant reduction in annexin V staining upon treatment with 5-FU + 3-MB-PP1 ($p \approx 0.0015$), but not nutlin-3 + 3-MB-PP1, whereas DR4 depletion did not significantly affect annexin V staining or

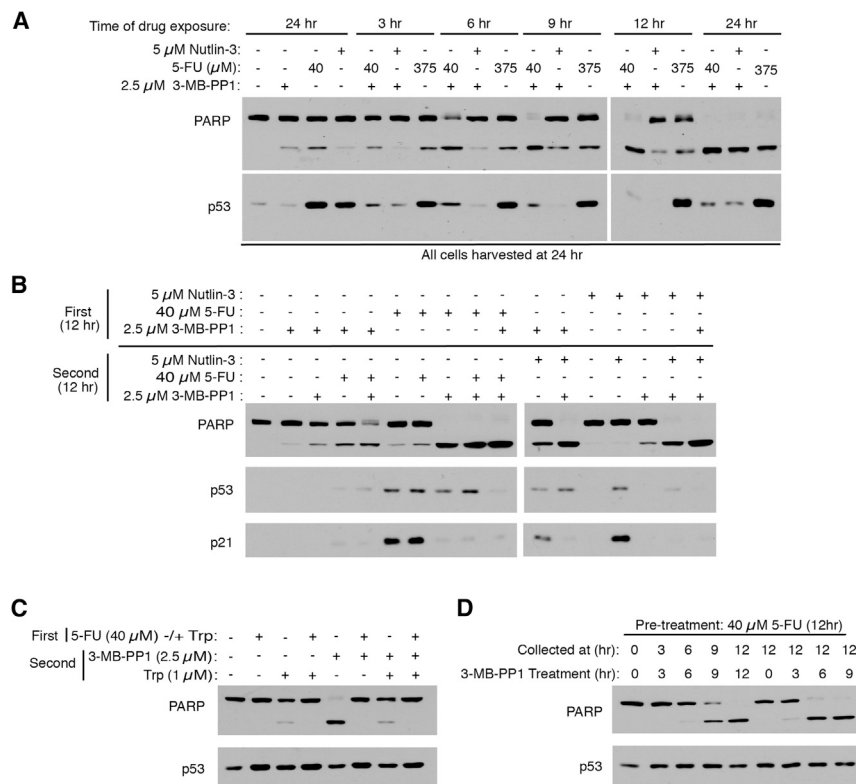


Figure 5. Cdk7 Inhibition after 5-FU Exposure Triggers Apoptosis Dependent on Transcription

(A) *CDK7^{as/as}* cells were treated with 5-FU, nutlin-3, and/or 3-MB-PP1, as indicated, for the indicated times. Where indicated, drug-containing media were removed and replaced with fresh, drug-free medium. All cells were harvested after 24 hr for extract preparation and immunoblot detection of PARP and p53.

(B) *CDK7^{as/as}* cells were incubated with the indicated drugs for 12 hr (first), washed, and incubated for an additional 12 hr with the indicated drugs (second), prior to extract preparation and immunoblot detection of PARP, p53, and p21.

(C) As in (B) but with the addition of 1 μ M triptolide (Trp) to the indicated cell populations, during either first or second incubation, as indicated.

(D) *CDK7^{as/as}* cells were pretreated with 40 μ M 5-FU for 12 hr, washed, treated with 2.5 μ M 3-MB-PP1 for the indicated times, and collected at the indicated times for extract preparation and immunoblot detection of PARP and p53.

PARP cleavage in response to either drug combination (Figures 7E, 7F, S6A, and S6B). Taken together, the results suggest repression of pro-survival p53 targets, with sparing of DR5 and activation of the extrinsic pathway, as a common mechanism through which Cdk7 inhibition can potentiate proapoptotic effects of 5-FU or switch cell fate from arrest to death in response to nutlin-3.

DISCUSSION

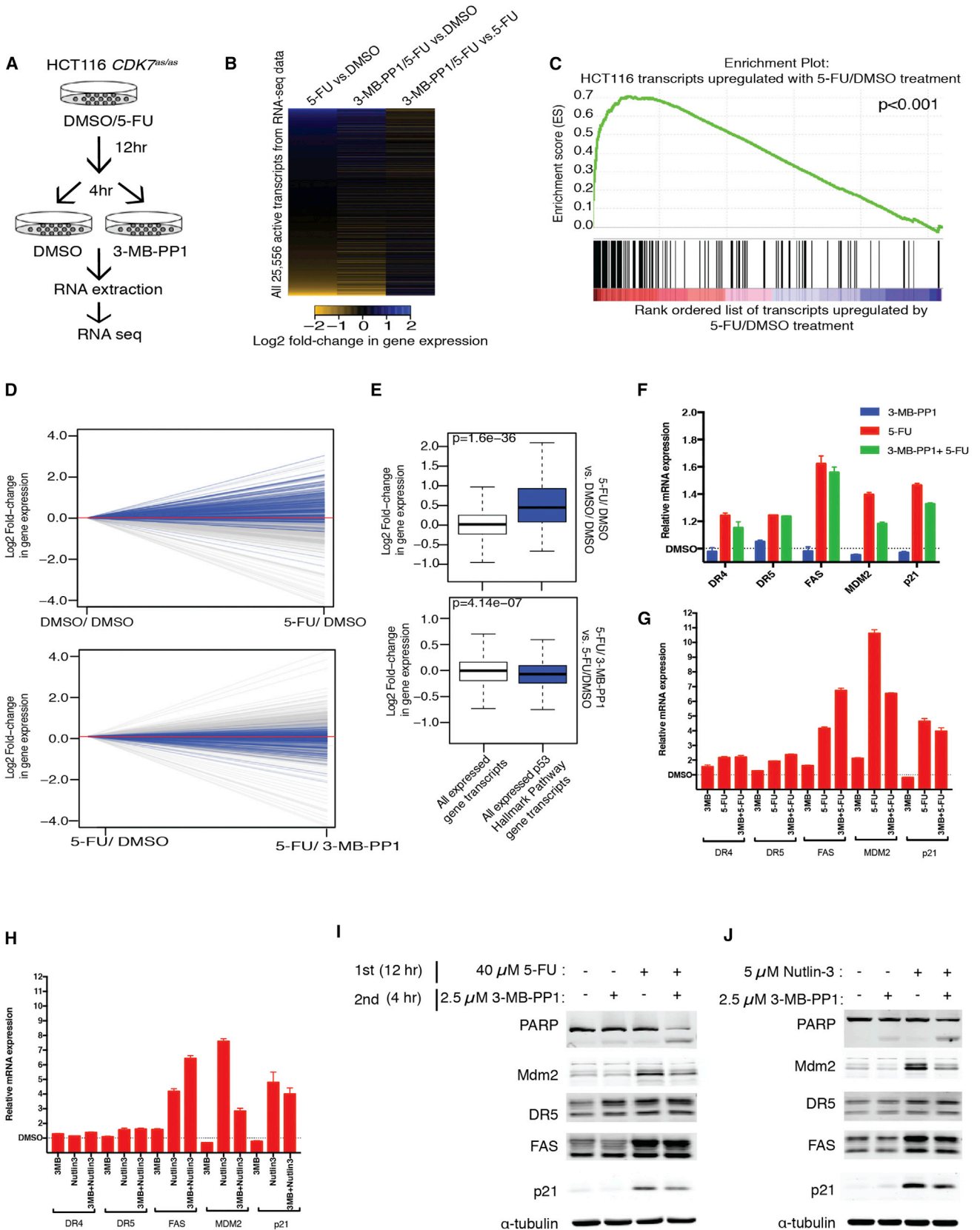
Protein kinases are attractive targets for drug discovery, but conservation of their active sites has hindered the development of selective small molecule inhibitors. Chemical genetics circumvents this limitation to facilitate mechanistic studies. Homozygous replacement of wild-type CDKs with AS variants in human cells enabled the dissection of complex biochemical pathways and identification of substrates of specific CDKs (Larochelle et al., 2007; Merrick et al., 2008, 2011; Wohlbold et al., 2012). Here we demonstrate the utility of AS kinase-expressing human cell lines as platforms for discovery of synthetic-lethal drug combinations.

Genetically sensitized cells also provide a benchmark by which to gauge drug specificity; the ability of THZ1 to recapitulate effects of 3-MB-PP1 in *CDK7^{as}* cells helped validate it as a Cdk7 inhibitor (Kwiatkowski et al., 2014). THZ1 treatment diminished bulk Ser2, Ser5, and Ser7 phosphorylation of the Pol II CTD whereas allele-specific inhibition of Cdk7^{as} did not (Larochelle et al., 2007; Glover-Cutter et al., 2009), suggesting that THZ1 had additional targets. THZ1 effects on both CTD phosphorylation and cell survival were, nevertheless, rescued by the expres-

sion of a THZ1-refractory Cdk7 variant (Kwiatkowski et al., 2014). To reconcile these results, we propose that Cdk7 inactivation is necessary but not sufficient; engagement of secondary targets such as Cdk12 and Cdk13—CTD kinases that can be selectively inhibited to trigger apoptosis (Zhang et al., 2016)—might contribute.

Irreversible inactivation of Cdk7 by THZ1 depends on covalent modification of Cys312, a residue outside the kinase domain conserved in Cdk12 and Cdk13 (Kwiatkowski et al., 2014). We now report THZ1 insensitivity of a Cdk7 variant with an active-site mutation. The resistance conferred by different mutations—F91G/D92E or C312S—indicates that specificity is determined by both the contours of the ATP-binding site and accessibility of a Cys residue for covalent modification (Kwiatkowski et al., 2014). Similar resistance to inhibitors of polo-like kinase 1 (Plk1) arose in human cells expressing an AS variant, due not to the gatekeeper mutation per se but rather to a second site substitution needed for mutant kinase activity (Burkard et al., 2012). The resistance of *CDK7^{as}* cells to THZ1 and YKL-1-116 provides a means to test whether phenotypes induced by these drugs depend on the inhibition of their primary target, and it suggests a potential path to acquired drug resistance in tumors.

As anti-cancer therapeutic targets, transcriptional CDKs did not offer the obvious advantage of being needed only in proliferating cells, and they seemed to entail a risk of toxicity to normal tissues. However, chemical-genetic ablation of Cdk7 catalytic function caused gene-specific rather than global repression of transcription in fission yeast (Viladevall et al., 2009) and human cells (this report). Although post-transcriptional mRNA stabilization might have masked more widespread effects on synthesis in budding yeast (Rodríguez-Molina et al., 2016), measurements of



(legend on next page)

Pol II occupancy likewise indicate differential requirements for Cdk7 at different genes (Glover-Cutter et al., 2009; Viladevall et al., 2009; Larochelle et al., 2012). Similarly, different mRNAs exhibit a range of sensitivities to THZ1 in human cells (Kwiatkowski et al., 2014). A common feature of several THZ1-hypersensitive tumors is dependence on super-enhancers—regulatory elements that nucleate high-density assembly of Pol II machinery and histone modifications permissive for high levels of transcription (Hnisz et al., 2013; Lovén et al., 2013). Reliance on oncogenic transcription factors—MYC in SCLC or neuroblastoma or RUNX1 in T-ALL (Chipumuro et al., 2014; Christensen et al., 2014; Kwiatkowski et al., 2014)—might make these tumors especially vulnerable to perturbation of the Pol II cycle. Hypersensitivity to THZ1 need not be based on addiction to a single factor, but it can be a cumulative effect of activating multiple, independent transcription programs, for example, in TNBC (Wang et al., 2015). Here we show that p53 activation in cancer cells can also induce dependence on Cdk7 function and might form the basis for a synthetic-lethal therapy (Figure 7G).

The balance between pro-apoptotic and pro-survival gene expression induced by p53—and thus the outcome of p53 activation—depends on the nature and strength of the p53-activating signal and varies among cell types exposed to the same stimulus (Donner et al., 2007). It is not clearly correlated, however, with levels of pro- versus anti-apoptotic gene transcription. Comparative analyses of responses to 5-FU or nutlin-3 implicated post-transcriptional stabilization of DR4, leading to caspase 8 activation and BID cleavage, in the killing of HCT116 cells by 5-FU (Henry et al., 2012). Conversely, RNAi-based screens identified signaling pathways that promote survival when p53 is activated by nutlin-3; depletion or inhibition of the kinases ATM or MET converted the response of HCT116 cells from division arrest to death, without gross alterations in gene expression patterns (Sullivan et al., 2012). Cdk7 inhibition achieves a similar cell fate switch through a transcriptional mechanism, which depends on the expression of *DR5*. The same p53 target con-

tributes to Cdk7 inhibitor-mediated, transcription-dependent potentiation of cell killing by 5-FU. Mechanistic studies will be needed to determine why *DR5* transcription is refractory to Cdk7 inhibition. Moreover, depletion of DR5 only partially suppressed synthetic lethality; although this might reflect incomplete knockdown, further analyses are warranted to reveal other pro-apoptotic p53 targets expressed (or anti-apoptotic ones repressed) in the presence of Cdk7 inhibitors.

Finally, comparison between THZ1 and YKL-1-116 suggests a rationale for enhancing selectivity of clinically important kinase inhibitors. Although the ability to inhibit multiple kinases might potentiate cell-killing effects of drugs such as THZ1 (Knight et al., 2010), it increases the risk of toxicity in normal tissues, and, as we have shown, it can limit efficacy in combinations with other agents. Whereas simultaneous inhibition of closely related targets can have additive or synergistic effects, other anti-targets might need to remain active to elicit a therapeutically desirable outcome, such as death of a cancer cell (Dar et al., 2012). We suggest that the organization of the transcription cycle, with precise coordination dependent on specialized functions of closely related CDKs, makes it uniquely susceptible to surgical inactivation of individual kinases that leaves others active to trigger maladaptive stress responses and death in vulnerable cell populations.

EXPERIMENTAL PROCEDURES

Cell Culture, Drug Treatment, and Extract Preparation

HCT116 cells were grown and lysates prepared as described (Larochelle et al., 2012). Cells were plated 24 hr prior to drug treatments. Synthesis and characterization of YKL-1-116 are described, and other drugs and antibodies used are listed, in the Supplemental Experimental Procedures.

Drug Synergy Analysis

Drug synergy was measured by Bliss independence analysis (Zhao et al., 2014) as described (Dhawan et al., 2016). Details of drug treatments and analysis are described in the Supplemental Experimental Procedures.

Figure 6. Cdk7 Inhibition Modulates the Transcriptional Response to p53 Activation

- (A) Schematic of sequential treatments of *CDK7^{as/as}* cells with 5-FU (40 μ M) and 3-MB-PP1 (2.5 μ M) used for RNA-seq analysis.
- (B) 5-FU treatment changes steady-state mRNA levels. HCT116 cells were treated as indicated in (A). Heatmaps display the Log₂ fold change in gene expression between the indicated conditions for the 25,556 transcripts expressed in DMSO.
- (C) Transcripts upregulated by 5-FU are enriched for p53 target genes. GSEA of all expressed transcripts rank-ordered from upregulated to downregulated following treatment with 5-FU is compared to transcripts associated with the p53 Hallmark Pathway Genes from MSigDB. GSEA-supplied p value < 0.001.
- (D) Per-transcript line plots showing Log₂ fold change in expression following 5-FU/DMSO in comparison to DMSO/DMSO treatment (top panel) and following 5-FU/3MB-PP1 in comparison to 5-FU/DMSO treatment (bottom panel). Gray lines indicate top 10% of most highly expressed gene transcripts in DMSO. Blue lines indicate p53 Hallmark Pathway Gene transcripts. Red line indicates no change in gene expression.
- (E) Boxplots showing distribution of Log₂ fold changes in expression for the indicated transcript sets following 5-FU/DMSO in comparison to DMSO/DMSO treatment (top panel) and following 5-FU/3MB-PP1 in comparison to 5-FU/DMSO treatment (bottom panel).
- (F) RNA-seq data for individual pro-apoptotic (*DR4*, *DR5*, and *FAS*) and pro-survival (*MDM2* and *p21*) p53 transcriptional targets, after the indicated drug treatments, relative to levels in DMSO (indicated by dashed horizontal line and defined as 1.0). Error bars indicate \pm SEM of biological replicates.
- (G) qRT-PCR analysis of selected p53 target gene expression in *CDK7^{as/as}* cells after simultaneous exposure to 5-FU and/or 3-MB-PP1, relative to levels in DMSO-treated cells. Error bars indicate \pm SEM of biological replicates.
- (H) qRT-PCR analysis of selected p53 target gene expression in *CDK7^{as/as}* cells after simultaneous treatment with nutlin-3 and/or 3-MB-PP1, relative to levels in DMSO-treated cells. Error bars indicate \pm SEM of biological replicates.
- (I) Immunoblot analysis of selected p53 target gene products in *CDK7^{as/as}* cells after sequential treatment with 5-FU and 3-MB-PP1. Cells were harvested 12 hr after exposure to the second drug (8 hr after second drug removal) for extract preparation and immunoblot detection of PARP, Mdm2, DR5, FAS, p21, and α -tubulin.
- (J) Immunoblot analysis of selected p53 target gene products in *CDK7^{as/as}* cells after simultaneous treatment with nutlin-3 and/or 3-MB-PP1. Cells were harvested after 12-hr drug exposure for extract preparation and immunoblot detection of PARP, Mdm2, DR5, FAS, p21, and α -tubulin.

See also Figure S5 and Table S3.

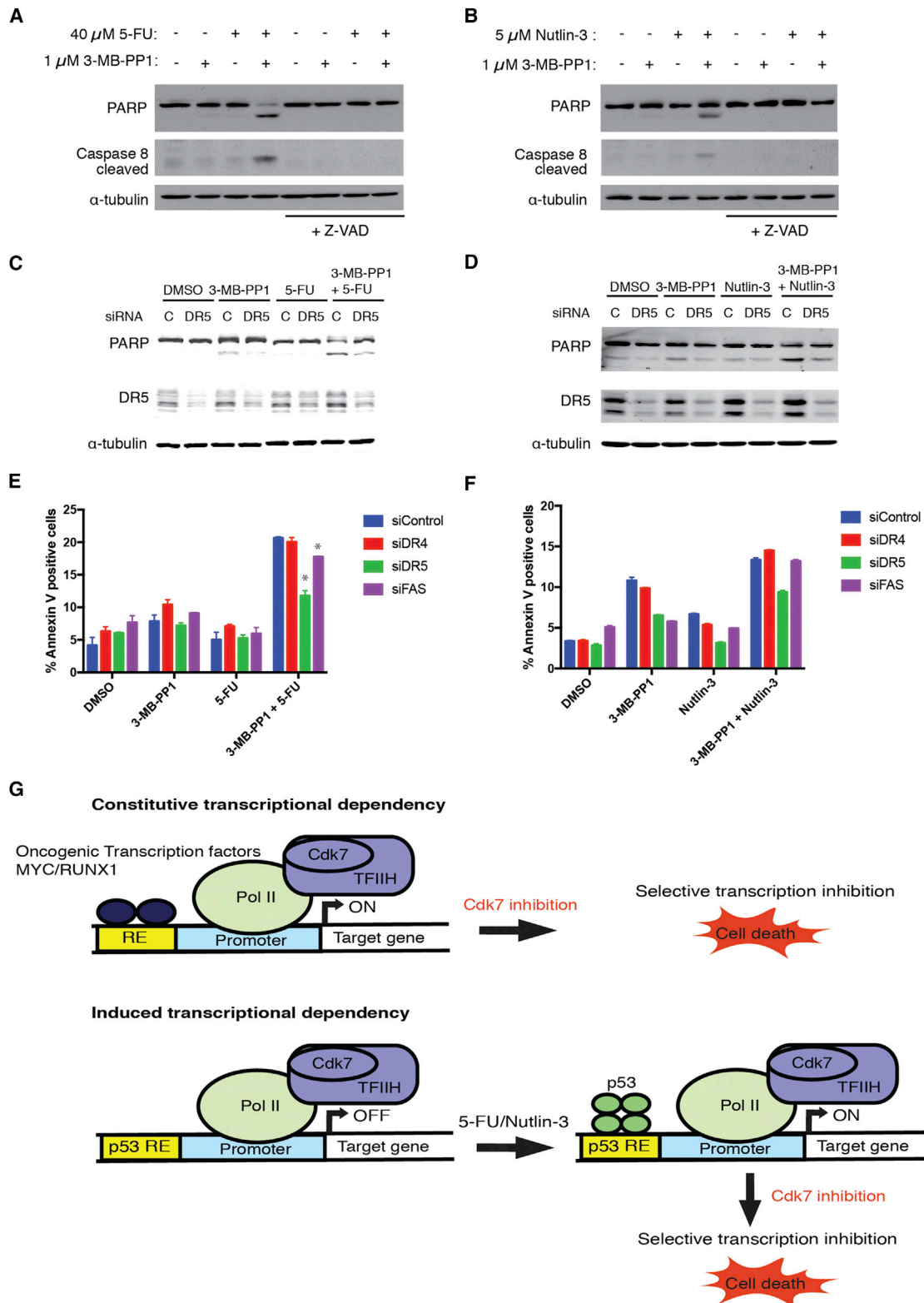


Figure 7. Activation of the Extrinsic Pathway of Apoptosis by Synthetic-Lethal Combinations of p53 Activators and Cdk7 Inhibitors, Dependent on DR5

(A) *CDK7^{as/as}* cells were treated with the indicated dose of 5-FU, with or without 1 μ M 3-MB-PP1 as indicated for 14 hr prior to extract preparation and immunoblot detection of PARP, activated caspase 8 (p18 isoform), and α -tubulin.

(legend continued on next page)

Kinase Assays

Kinase assays were performed with complexes of phosphorylated Cdk7 (WT or AS), cyclin H, and Mat1 generated by adding purified His-Mat1 to Cdk7-cyclin H dimer, as previously described (Larochelle et al., 2001), with or without treatment with various inhibitors, as described in the [Supplemental Experimental Procedures](#).

TP53 Knockout in *CDK7^{as/as}* Cells

The *TP53* gene was disrupted in HCT116 *CDK7^{as/as}* cells with an rAAV vector as described (Topaloglu et al., 2005).

RNA-Seq

RNA-seq reads were aligned to a version of the hg19 human reference genome with external RNA control consortium (ERCC) spike-in reference sequences added using tophat (Trapnell et al., 2009) version (v.)2.0.13 with parameters `-no-novel-juncs` and `-G` set to the human RefSeq transcript list downloaded in May 2013. Reads overlapping to the Encyclopedia of DNA Elements (ENCODE) list of blacklist regions (Consortium, 2012) were filtered using bedtools (Quinlan, 2014) `intersect`. Per-transcript expression values were created using RPKM_count.py from the RSeQC package (Wang et al., 2012) using `-e`, the RefSeq transcript list, and ERCC probe regions. Reads per kilobase of transcript per million mapped reads (RPKM) values between 0 and 0.1 were set to 0.1, and a pseudo-count of 0.1 was added to all transcripts. For each transcript, replicates of each condition were averaged. For displays, expressed transcripts are those with RPKM > 1 in the average of the DMSO replicates. GSEA (Subramanian et al., 2005) was performed with GSEA software, using the p53 Hallmark Pathway gene set from Broad Institute database MSigDB. This same gene set was used in all expression plots to indicate p53 pathway genes.

RNAi

Cells were transfected with siRNA oligonucleotides as described in the [Supplemental Experimental Procedures](#).

Data and Software Availability

The accession number for the sequencing data reported in this paper is GEO: GSE99794.

SUPPLEMENTAL INFORMATION

Supplemental Information includes six figures and three tables and can be found with this article online at <https://doi.org/10.1016/j.celrep.2017.09.056>.

AUTHOR CONTRIBUTIONS

S.K., R.A., M.M.S., N.K., B.J.A., S.L., R.A.Y., N.S.G., and R.P.F. designed experiments. S.K., R.A., M.M.S., N.K., B.J.A., Y.L., T.Z., C.M.O., and S.L. conducted experiments. S.K., R.A., N.K., B.J.A., and R.P.F. wrote the paper.

ACKNOWLEDGMENTS

We thank K.A. Merrick, M.B. Yaffe, and members of the Fisher lab for helpful discussions; C. Zhang and K. Shokat for 3-MB-PP1; F. Bunz for rAAV vector to disrupt *TP53*; N. Dhawan and A. Dar for advice on drug synergy assays; S. Mungamuri and S. Aaronson for help with flow cytometry; J.M. Espinosa for advice during early stages of this work; and A. Dar and K. Merrick for critical review of the manuscript. R.A. was supported by a Beatriu de Pinos fellowship of the Generalitat de Catalunya (2010 BP-A 00430). M.M.S. was supported by a fellowship from the NIH (T32 CA78207). B.J.A. is the Hope Funds for Cancer Research Grillo-Marxuach Family Fellow. This work was supported by NIH grants GM105773 and GM104291 to R.P.F., CA179483 to N.S.G., and HG002668 to R.A.Y. and by a grant from The Bridge Project, a partnership between the Koch Institute for Integrative Cancer Research at MIT and the Dana-Farber/Harvard Cancer Center to N.S.G. Flow cytometry was supported by support grant NIH (NCI) P30 CA196521 to the Tisch Cancer Institute. N.S.G., T.Z., and N.K. are inventors on a patent application covering THZ1, which is licensed to a company co-founded by N.S.G. and R.A.Y.

Received: May 8, 2017

Revised: August 21, 2017

Accepted: September 17, 2017

Published: October 10, 2017

REFERENCES

- Adelman, K., and Lis, J.T. (2012). Promoter-proximal pausing of RNA polymerase II: emerging roles in metazoans. *Nat. Rev. Genet.* *13*, 720–731.
- Bartkowiak, B., and Greenleaf, A.L. (2015). Expression, purification, and identification of associated proteins of the full-length hCDK12/CyclinK complex. *J. Biol. Chem.* *290*, 1786–1795.
- Bishop, A.C., Shah, K., Liu, Y., Witucki, L., Kung, C., and Shokat, K.M. (1998). Design of allele-specific inhibitors to probe protein kinase signaling. *Curr. Biol.* *8*, 257–266.
- Bösken, C.A., Farnung, L., Hintermair, C., Merzel Schachter, M., Vogel-Bachmayr, K., Blazek, D., Anand, K., Fisher, R.P., Eick, D., and Geyer, M. (2014). The structure and substrate specificity of human Cdk12/Cyclin K. *Nat. Commun.* *5*, 3505.
- Burkard, M.E., Santamaria, A., and Jallepalli, P.V. (2012). Enabling and disabling polo-like kinase 1 inhibition through chemical genetics. *ACS Chem. Biol.* *7*, 978–981.
- Can, G., Akpinar, B., Baran, Y., Zhivotovsky, B., and Olsson, M. (2013). 5-Fluorouracil signaling through a calcium-calmodulin-dependent pathway is required for p53 activation and apoptosis in colon carcinoma cells. *Oncogene* *32*, 4529–4538.
- Chao, S.H., and Price, D.H. (2001). Flavopiridol inactivates P-TEFb and blocks most RNA polymerase II transcription in vivo. *J. Biol. Chem.* *276*, 31793–31799.
- Chipumuro, E., Marco, E., Christensen, C.L., Kwiatkowski, N., Zhang, T., Hattaway, C.M., Abraham, B.J., Sharma, B., Yeung, C., Altshuler, A., et al. (2014).

(B) *CDK7^{as/as}* cells were treated with the indicated dose of 3-MB-PP1, with or without 5 μ M nutlin-3 as indicated for 14 hr prior to extract preparation and immunoblot detection of PARP, activated caspase 8 (p18 isoform), and α -tubulin.

(C) *CDK7^{as/as}* cells were transfected with siRNA targeting DR5 or control (scrambled) siRNA (C) and treated with the indicated drugs or drug combinations (doses: 40 μ M 5-FU and 1 μ M 3-MB-PP1) prior to lysis and immunoblot detection of PARP, DR5, and α -tubulin.

(D) *CDK7^{as/as}* cells were transfected with siRNA targeting DR5 or control (scrambled) siRNA (C), and treated with the indicated drugs or drug combinations (doses: 5 μ M nutlin-3 and 1 μ M 3-MB-PP1) prior to lysis and immunoblot detection of PARP, DR5, and α -tubulin.

(E) Quantification of annexin V-positive populations measured by flow cytometry in *CDK7^{as/as}* cells treated as in (C) (with the addition of cells transfected with siRNA targeting DR4 or FAS). Error bars indicate \pm SEM of three biological replicates. Statistically significant differences between knockdowns and controls are indicated (*).

(F) Quantification of annexin V-positive populations measured by flow cytometry in *CDK7^{as/as}* cells treated as in (D) (with the addition of cells transfected with siRNA targeting DR4 or FAS). Error bars indicate the range of values obtained in two biological replicates.

(G) Transcriptional dependency on Cdk7 activity induced by p53 stabilization mimics constitutive dependency due to constitutive transcriptional activation by oncogenic transcription factors such as MYC or RUNX1.

See also [Figure S6](#).

- CDK7 inhibition suppresses super-enhancer-linked oncogenic transcription in MYCN-driven cancer. *Cell* 159, 1126–1139.
- Christensen, C.L., Kwiatkowski, N., Abraham, B.J., Carretero, J., Al-Shahrour, F., Zhang, T., Chipumuro, E., Herter-Sprie, G.S., Akbay, E.A., Altabef, A., et al. (2014). Targeting transcriptional addictions in small cell lung cancer with a covalent CDK7 inhibitor. *Cancer Cell* 26, 909–922.
- Consortium, E.P.; ENCODE Project Consortium (2012). An integrated encyclopedia of DNA elements in the human genome. *Nature* 489, 57–74.
- Dar, A.C., Das, T.K., Shokat, K.M., and Cagan, R.L. (2012). Chemical genetic discovery of targets and anti-targets for cancer polypharmacology. *Nature* 486, 80–84.
- Dhawan, N.S., Scopton, A.P., and Dar, A.C. (2016). Small molecule stabilization of the KSR inactive state antagonizes oncogenic Ras signalling. *Nature* 537, 112–116.
- Donner, A.J., Hoover, J.M., Szostek, S.A., and Espinosa, J.M. (2007). Stimulus-specific transcriptional regulation within the p53 network. *Cell Cycle* 6, 2594–2598.
- Drygin, D., Lin, A., Bliesath, J., Ho, C.B., O'Brien, S.E., Proffitt, C., Omori, M., Haddach, M., Schwabe, M.K., Siddiqui-Jain, A., et al. (2011). Targeting RNA polymerase I with an oral small molecule CX-5461 inhibits ribosomal RNA synthesis and solid tumor growth. *Cancer Res.* 71, 1418–1430.
- Fisher, R.P. (2005). Secrets of a double agent: CDK7 in cell-cycle control and transcription. *J. Cell Sci.* 118, 5171–5180.
- Glover-Cutter, K., Larochelle, S., Erickson, B., Zhang, C., Shokat, K., Fisher, R.P., and Bentley, D.L. (2009). TFIIF-associated Cdk7 kinase functions in phosphorylation of C-terminal domain Ser7 residues, promoter-proximal pausing, and termination by RNA polymerase II. *Mol. Cell Biol.* 29, 5455–5464.
- Gray, N.S., Wodicka, L., Thunnissen, A.M., Norman, T.C., Kwon, S., Espinoza, F.H., Morgan, D.O., Barnes, G., LeClerc, S., Meijer, L., et al. (1998). Exploiting chemical libraries, structure, and genomics in the search for kinase inhibitors. *Science* 281, 533–538.
- Henry, R.E., Andrysk, Z., Paris, R., Galbraith, M.D., and Espinosa, J.M. (2012). A DR4:tBID axis drives the p53 apoptotic response by promoting oligomerization of poised BAX. *EMBO J.* 31, 1266–1278.
- Hnisz, D., Abraham, B.J., Lee, T.I., Lau, A., Saint-André, V., Sigova, A.A., Hoke, H.A., and Young, R.A. (2013). Super-enhancers in the control of cell identity and disease. *Cell* 155, 934–947.
- Johnson, N., Li, Y.C., Walton, Z.E., Cheng, K.A., Li, D., Rodig, S.J., Moreau, L.A., Unitt, C., Bronson, R.T., Thomas, H.D., et al. (2011). Compromised CDK1 activity sensitizes BRCA-proficient cancers to PARP inhibition. *Nat. Med.* 17, 875–882.
- Johnson, S.F., Cruz, C., Greifengberg, A.K., Dust, S., Stover, D.G., Chi, D., Primack, B., Cao, S., Bernhardt, A.J., Coulson, R., et al. (2016). CDK12 Inhibition Reverses De Novo and Acquired PARP Inhibitor Resistance in BRCA Wild-Type and Mutated Models of Triple-Negative Breast Cancer. *Cell Rep.* 17, 2367–2381.
- Knight, Z.A., Lin, H., and Shokat, K.M. (2010). Targeting the cancer kinome through polypharmacology. *Nat. Rev. Cancer* 10, 130–137.
- Kwiatkowski, N., Zhang, T., Rahl, P.B., Abraham, B.J., Reddy, J., Ficarro, S.B., Dastur, A., Amzallag, A., Ramaswamy, S., Tesar, B., et al. (2014). Targeting transcription regulation in cancer with a covalent CDK7 inhibitor. *Nature* 511, 616–620.
- Larochelle, S., Chen, J., Knights, R., Pandur, J., Morcillo, P., Erdjument-Bromage, H., Tempst, P., Suter, B., and Fisher, R.P. (2001). T-loop phosphorylation stabilizes the CDK7-cyclin H-MAT1 complex *in vivo* and regulates its CTD kinase activity. *EMBO J.* 20, 3749–3759.
- Larochelle, S., Merrick, K.A., Terret, M.E., Wohlbold, L., Barboza, N.M., Zhang, C., Shokat, K.M., Jallepalli, P.V., and Fisher, R.P. (2007). Requirements for Cdk7 in the assembly of Cdk1/cyclin B and activation of Cdk2 revealed by chemical genetics in human cells. *Mol. Cell* 25, 839–850.
- Larochelle, S., Amat, R., Glover-Cutter, K., Sansó, M., Zhang, C., Allen, J.J., Shokat, K.M., Bentley, D.L., and Fisher, R.P. (2012). Cyclin-dependent kinase control of the initiation-to-elongation switch of RNA polymerase II. *Nat. Struct. Mol. Biol.* 19, 1108–1115.
- Longley, D.B., Harkin, D.P., and Johnston, P.G. (2003). 5-fluorouracil: mechanisms of action and clinical strategies. *Nat. Rev. Cancer* 3, 330–338.
- Lovén, J., Hoke, H.A., Lin, C.Y., Lau, A., Orlando, D.A., Vakoc, C.R., Bradner, J.E., Lee, T.I., and Young, R.A. (2013). Selective inhibition of tumor oncogenes by disruption of super-enhancers. *Cell* 153, 320–334.
- Malumbres, M., and Barbacid, M. (2009). Cell cycle, CDKs and cancer: a changing paradigm. *Nat. Rev. Cancer* 9, 153–166.
- Merrick, K.A., Larochelle, S., Zhang, C., Allen, J.J., Shokat, K.M., and Fisher, R.P. (2008). Distinct activation pathways confer cyclin-binding specificity on Cdk1 and Cdk2 in human cells. *Mol. Cell* 32, 662–672.
- Merrick, K.A., Wohlbold, L., Zhang, C., Allen, J.J., Horiuchi, D., Huskey, N.E., Goga, A., Shokat, K.M., and Fisher, R.P. (2011). Switching Cdk2 on or off with small molecules to reveal requirements in human cell proliferation. *Mol. Cell* 42, 624–636.
- Morgan, D.O. (2007). *The Cell Cycle: Principles of Control* (London: New Science Press Ltd).
- Nilson, K.A., Guo, J., Turek, M.E., Brogie, J.E., Delaney, E., Luse, D.S., and Price, D.H. (2015). THZ1 Reveals Roles for Cdk7 in Co-transcriptional Capping and Pausing. *Mol. Cell* 59, 576–587.
- Peterlin, B.M., and Price, D.H. (2006). Controlling the elongation phase of transcription with P-TEFb. *Mol. Cell* 23, 297–305.
- Quinlan, A.R. (2014). BEDTools: The Swiss-Army Tool for Genome Feature Analysis. *Curr. Protoc. Bioinformatics* 47, 11.12.1–34.
- Ramanathan, Y., Rajpara, S.M., Reza, S.M., Lees, E., Shuman, S., Mathews, M.B., and Pe'ery, T. (2001). Three RNA polymerase II carboxyl-terminal domain kinases display distinct substrate preferences. *J. Biol. Chem.* 276, 10913–10920.
- Rodríguez-Molina, J.B., Tseng, S.C., Simonett, S.P., Taunton, J., and Ansari, A.Z. (2016). Engineered Covalent Inactivation of TFIIF-Kinase Reveals an Elongation Checkpoint and Results in Widespread mRNA Stabilization. *Mol. Cell* 63, 433–444.
- Sansó, M., and Fisher, R.P. (2013). Pause, play, repeat: CDKs push RNAP II's buttons. *Transcription* 4, 146–152.
- Schachter, M.M., Merrick, K.A., Larochelle, S., Hirschi, A., Zhang, C., Shokat, K.M., Rubin, S.M., and Fisher, R.P. (2013). A Cdk7-Cdk4 T-loop phosphorylation cascade promotes G1 progression. *Mol. Cell* 50, 250–260.
- Subramanian, A., Tamayo, P., Mootha, V.K., Mukherjee, S., Ebert, B.L., Gillette, M.A., Paulovich, A., Pomeroy, S.L., Golub, T.R., Lander, E.S., and Mesirov, J.P. (2005). Gene set enrichment analysis: a knowledge-based approach for interpreting genome-wide expression profiles. *Proc. Natl. Acad. Sci. USA* 102, 15545–15550.
- Sullivan, K.D., Padilla-Just, N., Henry, R.E., Porter, C.C., Kim, J., Tentler, J.J., Eckhardt, S.G., Tan, A.C., DeGregori, J., and Espinosa, J.M. (2012). ATM and MET kinases are synthetic lethal with nongenotoxic activation of p53. *Nat. Chem. Biol.* 8, 646–654.
- Titov, D.V., Gilman, B., He, Q.L., Bhat, S., Low, W.K., Dang, Y., Smeaton, M., Demain, A.L., Miller, P.S., Kugel, J.F., et al. (2011). XPB, a subunit of TFIIF, is a target of the natural product triptolide. *Nat. Chem. Biol.* 7, 182–188.
- Topaloglu, O., Hurley, P.J., Yildirim, O., Civin, C.I., and Bunz, F. (2005). Improved methods for the generation of human gene knockout and knockin cell lines. *Nucleic Acids Res.* 33, e158.
- Trapnell, C., Pachter, L., and Salzberg, S.L. (2009). TopHat: discovering splice junctions with RNA-Seq. *Bioinformatics* 25, 1105–1111.
- Vassilev, L.T., Vu, B.T., Graves, B., Carvajal, D., Podlaski, F., Filipovic, Z., Kong, N., Kammlott, U., Lukacs, C., Klein, C., et al. (2004). In vivo activation of the p53 pathway by small-molecule antagonists of MDM2. *Science* 303, 844–848.
- Viladevall, L., St Amour, C.V., Rosebrock, A., Schneider, S., Zhang, C., Allen, J.J., Shokat, K.M., Schwer, B., Leatherwood, J.K., and Fisher, R.P. (2009). TFIIF and P-TEFb coordinate transcription with capping enzyme recruitment at specific genes in fission yeast. *Mol. Cell* 33, 738–751.

- Wang, L., Wang, S., and Li, W. (2012). RSeQC: quality control of RNA-seq experiments. *Bioinformatics* *28*, 2184–2185.
- Wang, Y., Zhang, T., Kwiatkowski, N., Abraham, B.J., Lee, T.I., Xie, S., Yuzugullu, H., Von, T., Li, H., Lin, Z., et al. (2015). CDK7-dependent transcriptional addiction in triple-negative breast cancer. *Cell* *163*, 174–186.
- Wohlbold, L., Merrick, K.A., De, S., Amat, R., Kim, J.H., Larochelle, S., Allen, J.J., Zhang, C., Shokat, K.M., Petrini, J.H., and Fisher, R.P. (2012). Chemical genetics reveals a specific requirement for Cdk2 activity in the DNA damage response and identifies Nbs1 as a Cdk2 substrate in human cells. *PLoS Genet.* *8*, e1002935.
- Wu, L., Pan, J., Thoroddsen, V., Wysong, D.R., Blackman, R.K., Bulawa, C.E., Gould, A.E., Ocain, T.D., Dick, L.R., Errada, P., et al. (2003). Novel small-molecule inhibitors of RNA polymerase III. *Eukaryot. Cell* *2*, 256–264.
- Zhang, T., Kwiatkowski, N., Olson, C.M., Dixon-Clarke, S.E., Abraham, B.J., Greifenberg, A.K., Ficarro, S.B., Elkins, J.M., Liang, Y., Hannett, N.M., et al. (2016). Covalent targeting of remote cysteine residues to develop CDK12 and CDK13 inhibitors. *Nat. Chem. Biol.* *12*, 876–884.
- Zhao, W., Sachsenmeier, K., Zhang, L., Sult, E., Hollingsworth, R.E., and Yang, H. (2014). A New Bliss Independence Model to Analyze Drug Combination Data. *J. Biomol. Screen.* *19*, 817–821.